Analyzing the future climate change of Upper Blue Nile River basin using statistical downscaling techniques

Hydrology and earth system sciences
10.5194/hess-22-2391-2018

Dagnenet Fenta Mekonnen • Markus Disse

Introduction:

· The impact of climate change may be worse on transboundary rivers like the Upper Blue Nile River (UBNRB) where competition for water is becoming high from different economic, political and social interests of the riparian countries and when runoff variability of upstream countries can greatly affect the downstream countries.

· The objective of this study is (i) to evaluate the comparative performance of two widely used statistical downscaling Model (SDSM) over the UBNRB, and (ii) to downscale future climate scenarios of precipitation, maximum temperature (Tmax) and minimum temperature (Tmin) at acceptable spatial and temporal resolution, which can be used directly for further hydrological impact studies.

Data and methods:

· from 7°45′ to 13° N and 34°30′ and 37°45′ E .

· 45% of the countries surface water resources, 20% of the population, 17% of the landmass, 40% of the nation's agricultural product and a large portion of the hydropower and irrigation potential of the country.

· Observed data: Ethiopian Meteorological Agency (EMA), 15 rainfall and 25 temperature stations.

· GCMs:

- LARS WG:

Table 1. Selected global climate models from IPCC AR4 incorporated into LARS-WG.

Research center	Country	GCM	Model acronym	Grid resolution	Emission scenarios	Time periods
Common Wealth Scientific and Industrial Research Organization	Australia	CSIRO-MK3	CSMK3	1.9° × 1.9°	A1B, B1	B, T1, T2, T3
Max-Plank Institute for Meteorology	Germany	ECHAM5-OM	MPEH5	1.9° × 1.9°	A1B, A2, B1	B, T1, T2, T3
National Institute for Environmental Studies	Japan	MRI-CGCM2.3.	MIHR	2.8° × 2.8°	A1B, B1	B, T1, T2, T3
UK Meteorological Office	UK	HadCM3	HADCM3	2.5° × 3.75°	A1B, A2, B1	B, T1, T2, T3
Geophysical Fluid Dynamics Lab	USA	GFDL-CM2.1	GFCM21	2° × 2.5°	A1B, A2, B1	B, T1, T2, T3
National Centre for Atmospheric Research	USA	CCSM3	NCCCS	1.4° × 1.4°	A1B, B1	B, T1, T2, T3

B: baseline; T1: 2011–2030; T2: 2046–2065; T3: 2081–2100

- SDSM: HadCM3 (2.5◦ x 3.75◦) and canESM2 (2.5◦ x 2.5◦)

· Periods: 1984-1995, 1996-2001 and 2006-2100

· Methods: LARS WG (weather generator) and SDSM

` RMSE, Bias, MAE

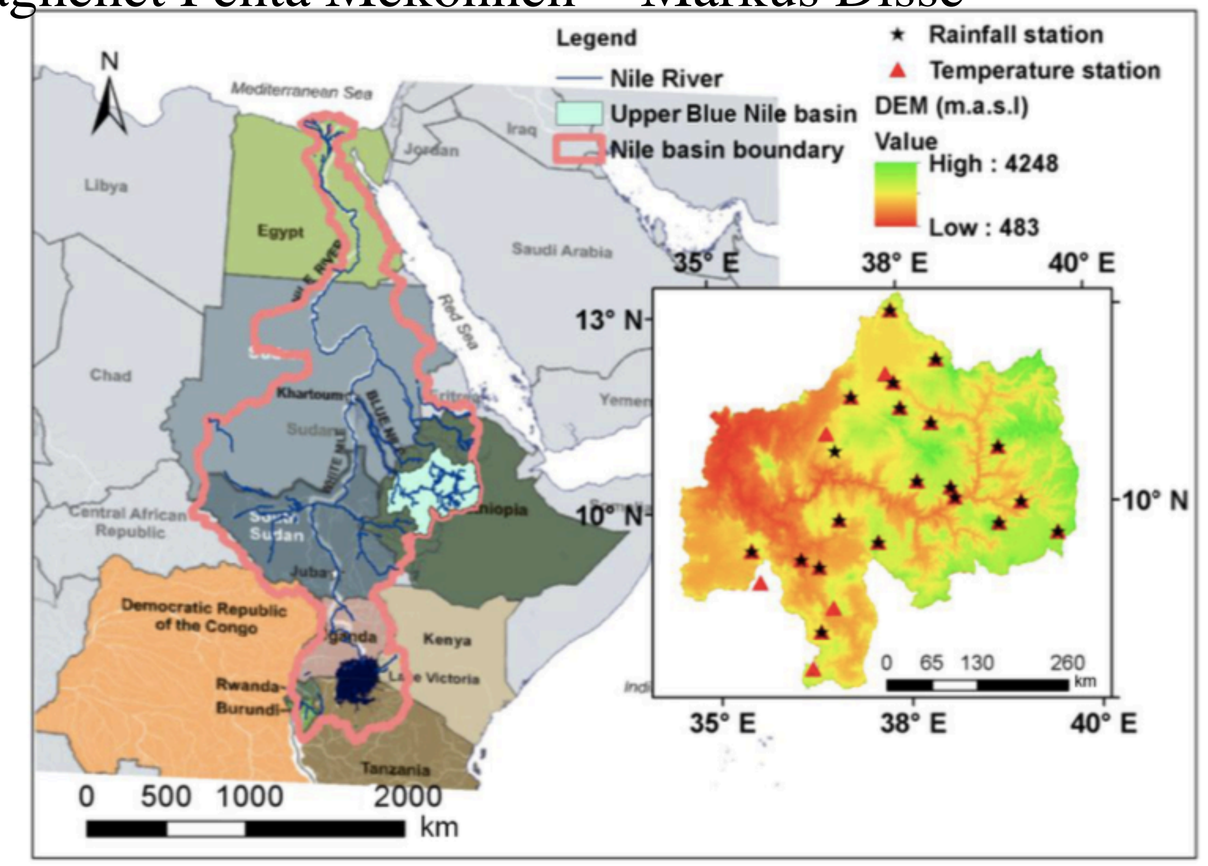

Figure 1. Location map of the study area.

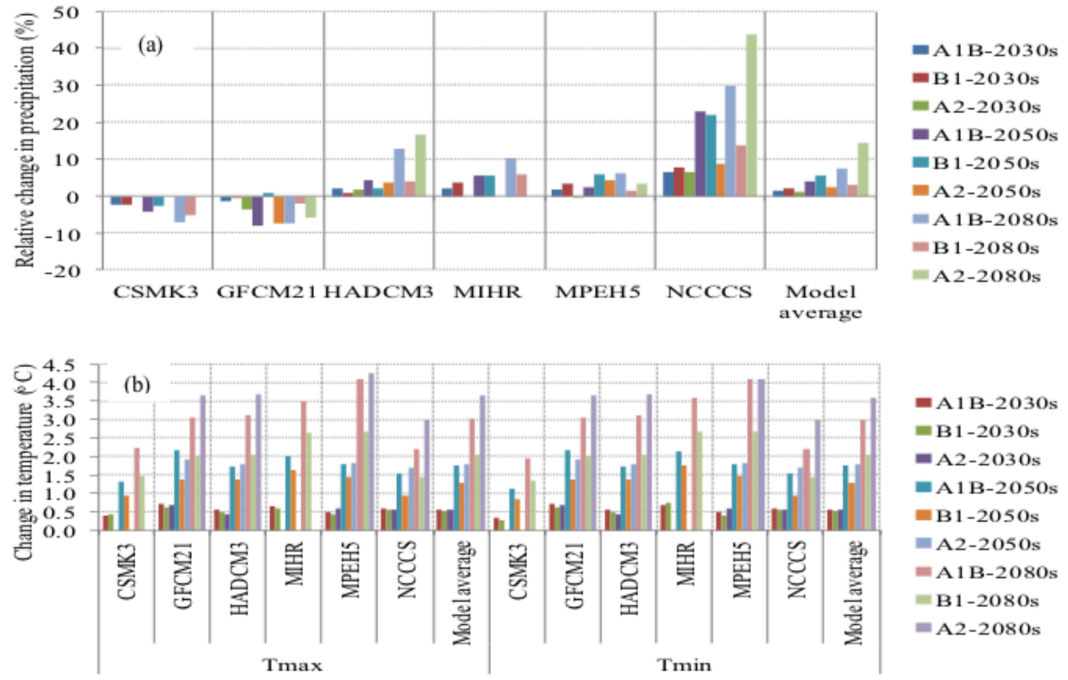

Figure 4. (a) Relative change mean annual precipitation and **(b)** change in T_{max} and T_{min} modeled from six GCMs for three time periods of UBNRB compared from the reference period of 1984–2011 by using LARS-WG.

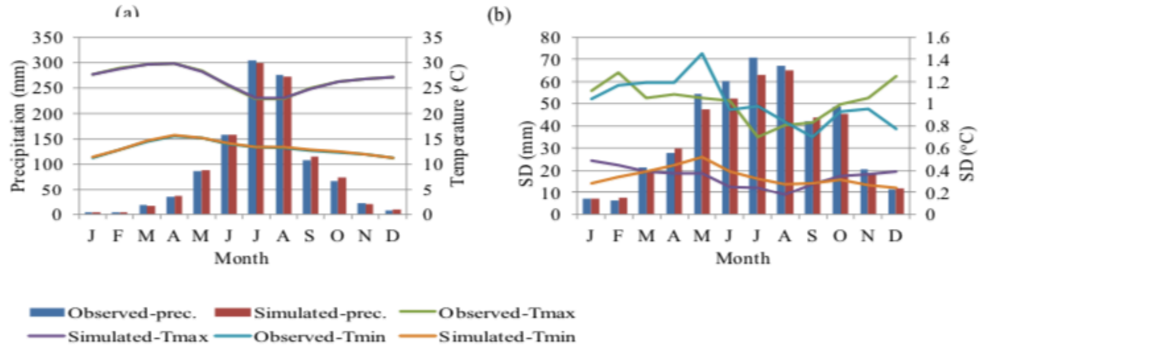

Figure 3. Observed and simulated **(a)** mean monthly precipitation, T_{max} and T_{min}; **(b)** standard deviation of precipitation, T_{max} and T_{min} using LARS-WG.

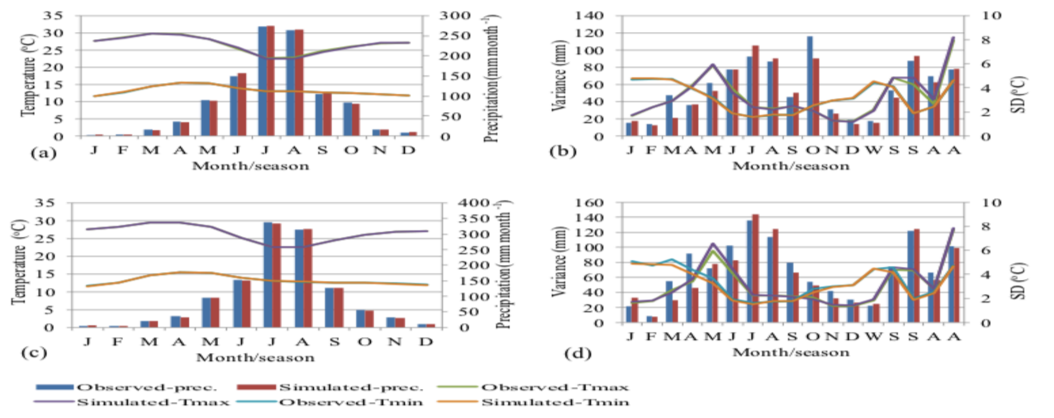

Figure 6. Calibration of observed and simulated of precipitation, maximum temperature and minimum temperature for the Gondar station using SDSM from canESM2 and HadCM3 from **(a, b)** to **(c, d)**.

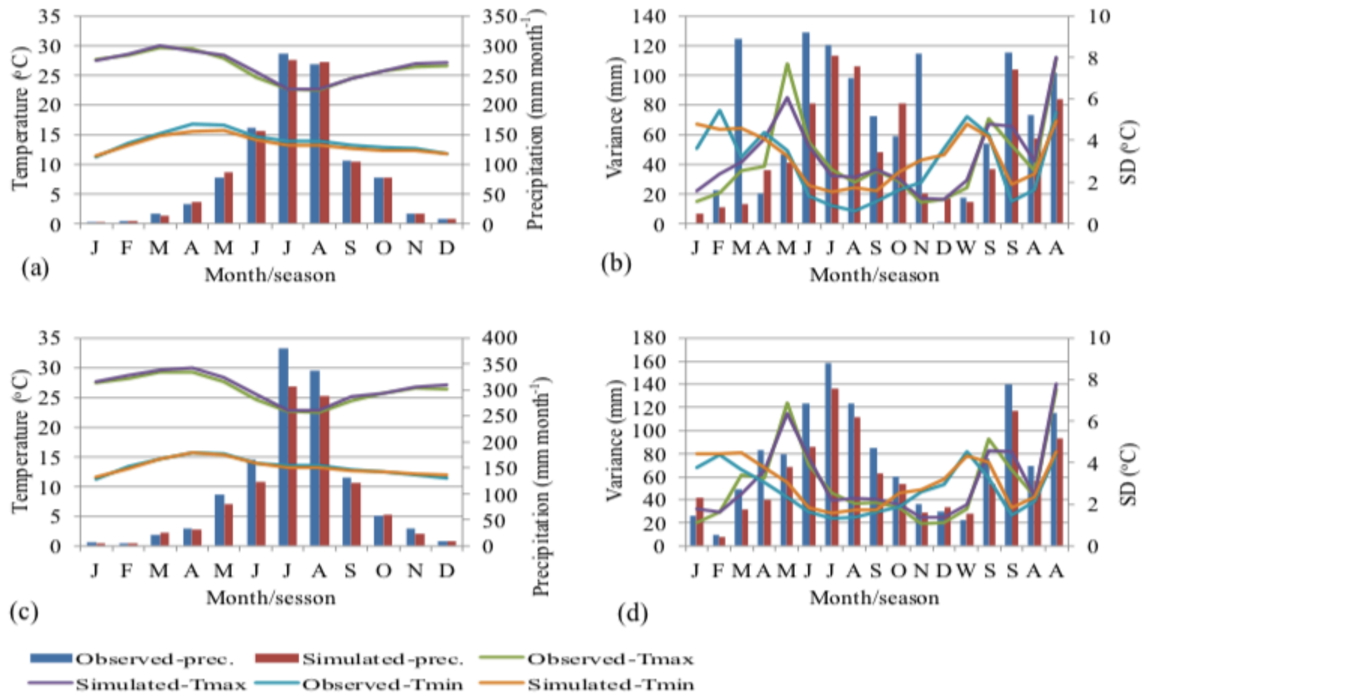

Figure 7. Validation of observed and simulated of precipitation, maximum temperature and minimum temperature for Gondar station using SDSM from canESM2 and HadCM3 from **(a, b)** to **(c, d)** respectively.

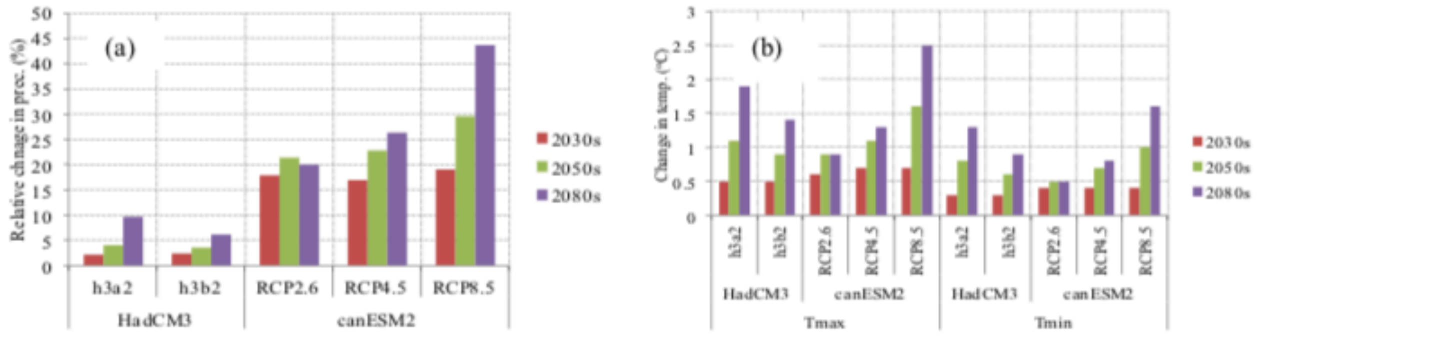

Figure 8. (a) Relative change of mean annual precipitation, and **(b)** change of mean annual T_{max} and T_{min} for three time periods compared to the baseline period of UBNRB using SDSM for HadCM3 and canESM2 GCMs under different scenarios.

Conclusions:

· The results suggested that SDSMusing canESM2 GCM captures the long-term monthly average very well at most of the stations. (CMIP5 GCMs performs better than CMIP3 GCMs)

· SDSM using the canESM2 CMIP5 GCM was able to reproduce more accurate long-term mean monthly precipitation.

· LARS-WG performed best in qualitative measures in capturing the distribution and extreme events of the daily precipitation than SDSM.

2020/10/22

Comparison of artificial neural network and multivariate linear regression methods for estimation of daily soil temperature in an arid region

Meteorology and atmospheric physics
10.1007/s00703-010-0110-z

Hossein Tabari • Ali-Akbar Sabziparvar · Mohammad Ahmadi

Introduction:

· Soil temperature (Ts) is an important parameter in different areas of research such as hydrology, soil science, geotechnology, ecology, meteorology, agronomy and environmental studies.

· The temperature regimes of the soil surface have two cyclical periods, namely diurnal and annual cycles.

- The variations of soil temperature resulting from daytime heating and nighttime cooling are known as diurnal variations.
- The annual variations in Ts result from the variations in short-wave radiation throughout the year.

· Soil temperature is influenced by a number of meteorological factors (e.g., solar radiation, air temperature, etc.), site topography, soil water content, soil texture and the area of surface covered by litter and canopies of plants.

Data and methods:

· Isfahan Province, located in the central part of Iran, from 49°36′ E to 55°31′ E longitude and 30°42′ N and 34°27′ N latitude.

·The climate of Isfahan is classified as arid, experiencing warm weather in summer and cold in winter. The largest and the most arid desert land (Lut) of Iran, which lies on the eastern parts of Isfahan, affects the climate condition of this province.

· The average air temperature in this province is 19.3°C in spring, 27.2°C in summer, 12.4°C in autumn and 5.7°C in winter.

· Periods: 1996-2005

· Methods: MLP and MLR

` RMSE, r, MAE depths of 5, 10, 20, 30, 50 and 100 cm

Table 1 Geographic characteristics of the synoptic stations used in the study

Stations	Longitude (E)	Latitude (N)	Elevation (m)
Kashan	51°27′	33°59′	982
Isfahan	51°40′	32°37′	1,550
Shahreza	51°50′	31°59′	1,845
Natanz	51°54′	33°32′	1,685
Naein	53°5′	32°51′	1,549

Fig. 2 Monthly means of daily precipitation (mm), air temperature (°C), relative humidity (%) and solar radiation (MJ m^{-2} day^{-1}) in the study area

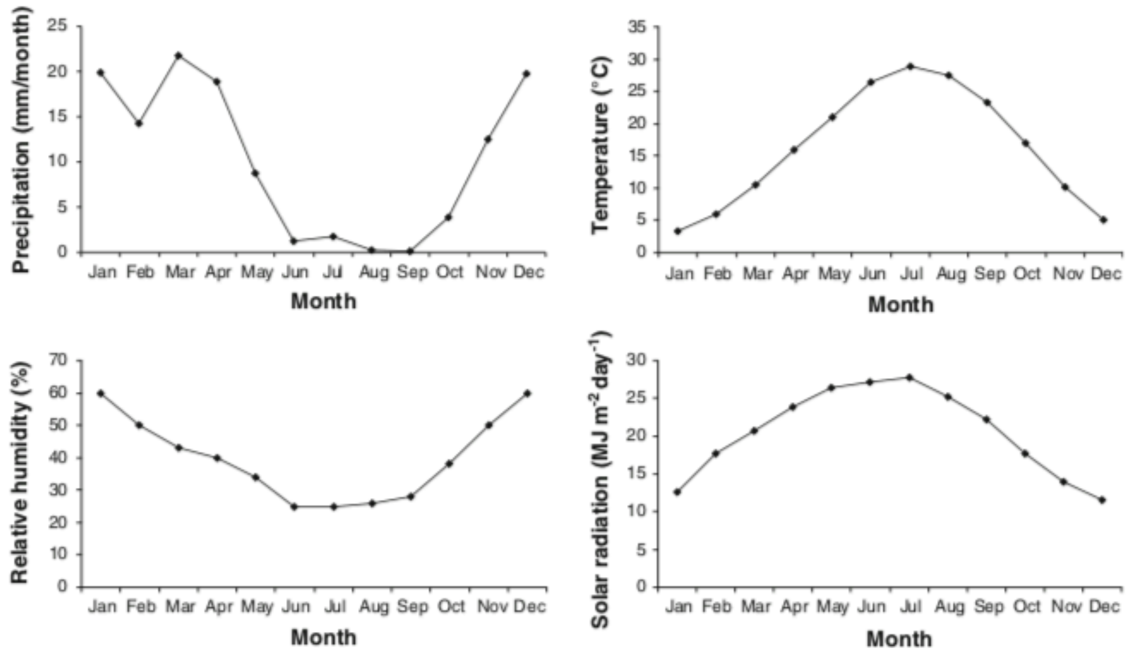

Sigmoid, Tanh and Linear (activation functions) & Levenberg-Marquardt, Delta-bar-Delta, Step, Momentum, ConjugateGradient and Quickpoop (learning algorithms)

Fig. 3 Architecture of the neural network model used in this study

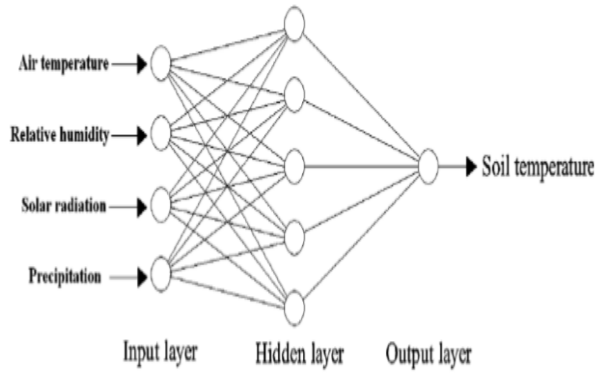

Table 5 Statistical performance evaluation criteria of MLR for all depths

Soil depth (cm)	r	RMSE	MAE	Equation
5	0.99	1.474	1.062	$T_{S\text{-}5} = 1.233T_a - 0.411RH + 0.004R_S - 0.143P + 0.585$
10	0.99	1.532	1.918	$T_{S\text{-}10} = 1.194T_a - 0.167RH + 0.017R_S - 0.109P + 0.526$
20	0.98	1.634	2.106	$T_{S\text{-}20} = 1.087T_a + 1.472RH + 0.001R_S - 0.088P + 0.896$
30	0.97	1.830	2.114	$T_{S\text{-}30} = 1.052T_a + 2.505RH - 0.006R_S - 0.118P + 1.332$
50	0.95	2.110	2.382	$T_{S\text{-}50} = 0.916T_a + 4.038RH - 0.009R_S - 0.176P + 3.734$
100	0.87	2.446	2.752	$T_{S\text{-}100} = 0.661T_a + 5.977RH + 7.17 \times 10^{-5}R_S - 0.244P + 7.288$

* RMSE and MAE are in °C

Fig. 1 Location of Isfahan Province and the synoptic stations

Table 4 Statistical performance evaluation criteria of ANN for all depths in training and testing phases

Soil depth (cm)	Training phase			Testing phase		
	r	RMSE	MAE	r	RMSE	MAE
5	0.99	0.221	0.351	0.99	0.432	0.624
10	0.98	0.325	0.457	0.98	0.547	0.786
20	0.98	0.472	0.628	0.97	0.654	0.859
30	0.98	0.593	0.791	0.96	0.728	0.931
50	0.97	0.712	0.988	0.96	0.975	1.211
100	0.97	1.021	1.312	0.95	1.125	1.425

* RMSE and MAE are in °C

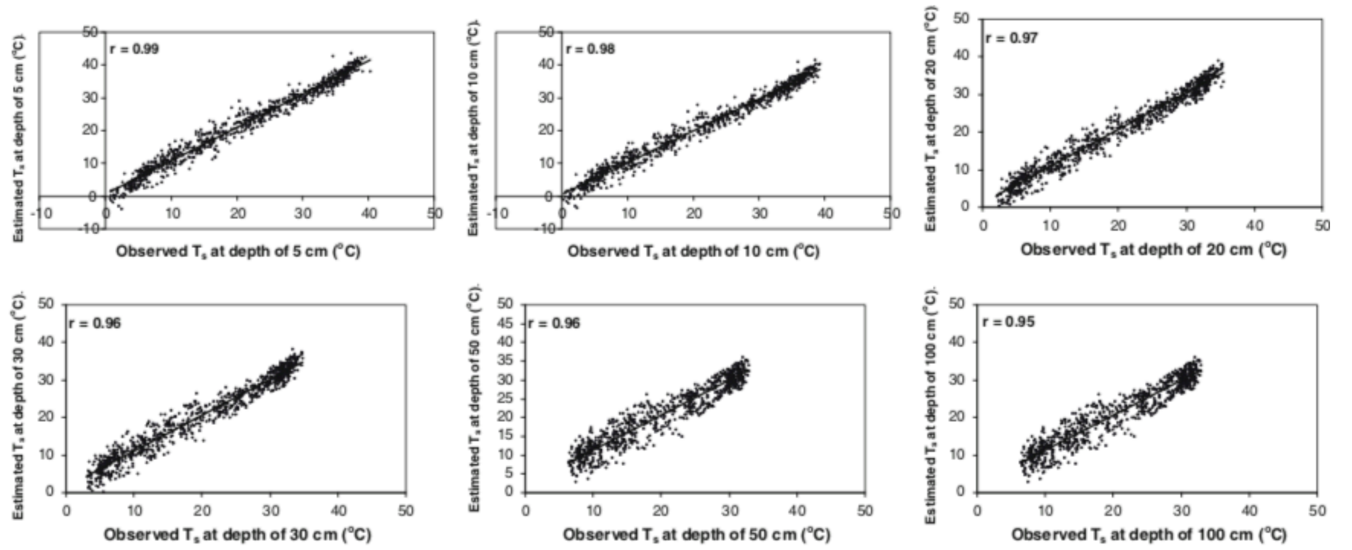

Fig. 5 Comparison of the daily T_S predicted by ANN and observed values at the testing phase

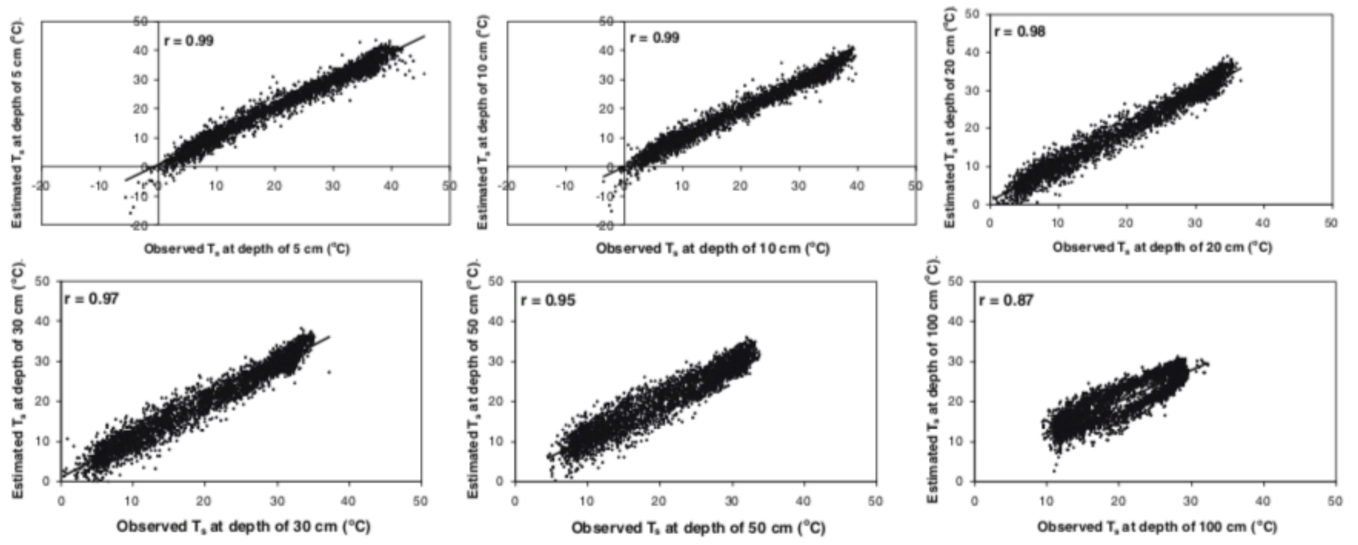

Fig. 6 Comparison of the daily T_S predicted by MLR and observed values at different depths

Conclusions:

· The 4-5-1 architecture produced the best results and the Levenberg-Marquardt learning algorithm and Sigmoid activation function were found to be the most appropriate choices for the estimations.

· An increase in the number of hidden layers and the number of neurons in the hidden layer produced no significant improvement in the Ts forecast.

· MLR was able to predict Ts at a desirable level of accuracy, but ANN was more suitable than MLR for estimation of daily Ts at different depths in the selected arid study site.

· The most effective parameters influencing Ts at different depths were Ta and RH, respectively.